PROCEEDINGS A

rspa.royalsocietypublishing.org

Research

Cite this article: Van Gorder RA. 2015 The Biot–Savart description of Kelvin waves on a quantum vortex filament in the presence of mutual friction and a driving fluid. *Proc. R. Soc. A* **471**: 20150149.
http://dx.doi.org/10.1098/rspa.2015.0149

Received: 4 March 2015
Accepted: 3 June 2015

Subject Areas:
low temperature physics, wave motion, mathematical physics

Keywords:
quantum vortex dynamics, superfluid Helium, non-locality, Donnelly–Glaberson instability, Kelvin waves, mutual friction

Author for correspondence:
Robert A. Van Gorder
e-mail: Robert.VanGorder@maths.ox.ac.uk

The Biot–Savart description of Kelvin waves on a quantum vortex filament in the presence of mutual friction and a driving fluid

Robert A. Van Gorder

Mathematical Institute, University of Oxford, Andrew Wiles Building, Radcliffe Observatory Quarter, Woodstock Road, Oxford OX2 6GG, UK

We study the dynamics of Kelvin waves along a quantum vortex filament in the presence of mutual friction and a driving fluid while taking into account non-local effects due to Biot–Savart integrals. The Schwarz model reduces to a nonlinear and non-local dynamical system of dimension three, the solutions of which determine the translational and rotational motion of the Kelvin waves, as well as the amplification or decay of such waves. We determine the possible qualitative behaviours of the resulting Kelvin waves. It is well known from experimental and theoretical studies that the Donnelly–Glaberson instability plays a role on the amplification or decay of Kelvin waves in the presence of a driving normal fluid velocity, and we obtain the relevant stability criterion for the non-local model. While the stability criterion is the same for local and non-local models when the wavenumber is sufficiently small, we show that large differences emerge for the large wavenumber case (tightly coiled helices). The results demonstrate that non-local effects have a stabilizing effect on the Kelvin waves, and hence larger normal fluid velocities are required for amplification of large wavenumber Kelvin waves. Additional qualitative differences between the local and non-local models are explored.

1. Introduction and model formulation

The mathematical formulation for the self-induced motion of a thin vortex filament was given by Da Rios [1] and rediscovered by others later [2,3]. The dynamics

THE ROYAL SOCIETY PUBLISHING

of such a classical [4] or low-temperature quantum [5] vortex filament are governed by the Biot–Savart law

$$\mathbf{r}_t = \frac{\Gamma}{4\pi}\int_\ell \frac{(\mathbf{s}-\mathbf{r})\times \mathrm{d}\mathbf{s}}{|\mathbf{s}-\mathbf{r}|^3} = \frac{\Gamma}{4\pi}\,\mathrm{BS}[\mathbf{r}], \tag{1.1}$$

where curve $\mathbf{r}$ represents the spatial curve modelling the vortex filament at any time t, Γ denotes the strength of the filament (circulation), and ℓ is the path along which the filament lies. This representation is non-local, meaning that distant parts of the filament can affect the behaviour of the filament at a specific point. As this equation is non-local, it is difficult to solve for most vortex configurations. Still, a number of approximations of both analytical and numerical flavours have been discovered. The difficulty and usefulness of such approximation methods will depend strongly on the type of filament solution sought. Due to the mathematical and computational difficulties in studying (1.1), the local induction approximation (LIA) is sometimes used to replace the integral in (1.1) with a far simpler relation, viz.,

$$\mathbf{r}_t = 2\frac{\Gamma}{4\pi}\ln\left(\frac{1}{\epsilon}\right)\kappa\mathbf{t}\times\mathbf{n} = \frac{\Gamma}{2\pi}\ln\left(\frac{1}{\epsilon}\right)\mathrm{LIA}[\mathbf{r}], \tag{1.2}$$

where $\mathbf{t}$ is the tangent vector, $\mathbf{n}$ is the normal vector to $\mathbf{r}$, and κ is the scalar curvature. Here, ϵ is a small distance parameter signifying that we have removed the logarithmic singularity and are approximating the region near this singularity. The right-hand side of (1.2) is the binormal vector (up to scaling). While (1.2) defines a nonlinear vector partial differential equation, its solution is still simpler than that of the non-local and singular equation (1.1). The LIA is useful when the vortex filaments are very thin, which is true for instance in the case of quantized vortex filaments in superfluid helium. For classical vortex filaments, the LIA has well-known limitations. Therefore, it is certainly desirable to be able to study solutions of (1.1) in the context of quantum vortex filaments, to identify the qualitative effects of including non-locality.

In the case of a quantum vortex filament, the Schwarz model [6] takes into account normal fluid velocity and mutual friction terms, which were previously shown to be of relevance in studies on superfluid Helium [7,8]. In the non-local formulation, this reads

$$\mathbf{r}_t = \frac{\Gamma}{4\pi}\,\mathrm{BS}[\mathbf{r}] + \alpha\mathbf{t}\times\left(\mathbf{U}-\frac{\Gamma}{4\pi}\,\mathrm{BS}[\mathbf{r}]\right) - \alpha'\mathbf{t}\times\left(\mathbf{t}\times\left(\mathbf{U}-\frac{\Gamma}{4\pi}\,\mathrm{BS}[\mathbf{r}]\right)\right). \tag{1.3}$$

Often times, this model is given in local form by replacement of the Biot–Savart operators with the local LIA operators, resulting in the quantum LIA:

$$\begin{aligned}\mathbf{r}_t = {}& \frac{\Gamma}{2\pi}\ln(\epsilon^{-1})\,\mathrm{LIA}[\mathbf{r}] + \alpha\mathbf{t}\times\left(\mathbf{U}-\frac{\Gamma}{2\pi}\ln(\epsilon^{-1})\,\mathrm{LIA}[\mathbf{r}]\right) - \alpha'\mathbf{t}\\ &\times\left(\mathbf{t}\times\left(\mathbf{U}-\frac{\Gamma}{2\pi}\ln(\epsilon^{-1})\,\mathrm{LIA}[\mathbf{r}]\right)\right).\end{aligned} \tag{1.4}$$

It is also possible to use the local approximation near the core of the vortex filament while keeping non-local effects away from the core. This approximation method has been suggested and used in numerical studies of superfluid vortex filament dynamics [6], and the appeal of this method is that it permits one to directly compare the LIA solutions with the Biot–Savart solutions. In this way, one can determine the influence of non-locality on a vortex filament. This approach gives useful analytical information about the time evolution of helical vortex filaments under the Biot–Savart dynamics.

Introducing the regularized Biot–Savart integral operator

$$\mathrm{BS}_\epsilon[\mathbf{r}] = 2\ln\left(\frac{1}{\epsilon}\right)\mathrm{LIA}[\mathbf{r}] + \int_{|\mathbf{s}-\mathbf{r}|>\epsilon}\frac{(\mathbf{s}-\mathbf{r})\times\mathrm{d}\mathbf{s}}{|\mathbf{s}-\mathbf{r}|^3}, \tag{1.5}$$

we obtain a regularized version of the non-local form of the Schwarz model

$$\mathbf{r}_t = \frac{\Gamma}{4\pi}\,\mathrm{BS}_\epsilon[\mathbf{r}] + \alpha\mathbf{t}\times\left(\mathbf{U}-\frac{\Gamma}{4\pi}\,\mathrm{BS}_\epsilon[\mathbf{r}]\right) - \alpha'\mathbf{t}\times\left(\mathbf{t}\times\left(\mathbf{U}-\frac{\Gamma}{4\pi}\,\mathrm{BS}_\epsilon[\mathbf{r}]\right)\right). \tag{1.6}$$

If we scale both time and the normal fluid velocity like

$$t \mapsto \frac{\Gamma}{2\pi}\ln(\epsilon^{-1})t \quad \text{and} \quad \mathbf{U} \mapsto \frac{\Gamma}{2\pi}\ln(\epsilon^{-1})\mathbf{U}, \tag{1.7}$$

we obtain the quantum LIA with non-local corrections,

$$\mathbf{r}_t = \mathrm{qBS}[\mathbf{r}], \tag{1.8}$$

where the integro-differential operator qBS[**r**] can be partitioned into a local part (involving space derivatives) and a non-local part (involving space integrals) like

$$\begin{aligned}\mathrm{qBS}[\mathbf{r}] = {} & \kappa\mathbf{t}\times\mathbf{n} + \alpha\mathbf{t}\times(\mathbf{U} - \kappa\mathbf{t}\times\mathbf{n}) - \alpha'\mathbf{t}\times\{\mathbf{t}\times(\mathbf{U} - \kappa\mathbf{t}\times\mathbf{n})\} \\ & + \frac{\lambda}{2}\{\mathbf{I}_\epsilon[\mathbf{r}] - \alpha\mathbf{t}\times\mathbf{I}_\epsilon[\mathbf{r}] + \alpha'\mathbf{t}\times(\mathbf{t}\times\mathbf{I}_\epsilon[\mathbf{r}])\}.\end{aligned} \tag{1.9}$$

Here, $\mathbf{I}_\epsilon[\mathbf{r}]$ denotes the regularized integral operator

$$\mathbf{I}_\epsilon[\mathbf{r}] = \int_{|\mathbf{s}-\mathbf{r}|>\epsilon} \frac{(\mathbf{s}-\mathbf{r})\times \mathrm{d}\mathbf{s}}{|\mathbf{s}-\mathbf{r}|^3}, \tag{1.10}$$

whereas the constant λ denotes the scaling of the logarithmic constant, $\lambda = 1/\ln(\epsilon^{-1})$. When $\lambda = 0$, we recover the scaled form of the quantum LIA, which has been studied often in the literature. When $\lambda \neq 0$, we obtain the non-local corrections to the quantum LIA. Alternately, when α and α' are taken to zero, we recover the regularized Biot–Savart dynamics. Therefore, the time evolution of a vortex filament under (1.8) holds both quantum and non-local effects.

Regarding helical filaments, the 'cut-off' method based on the oscillating vortex ring has been employed to the study of helical vortex filaments [4]. This method also approximates the inner region of the vortex cross section. Under appropriate assumptions, the method reduces to the LIA. An analysis of the approach was conducted by Moore & Saffman [9,10]. Using the 'cut-off' method, Ricca [11] obtained analytical results in the small helix diameter and large torsion limit, and demonstrated that torsion strongly influences the motion of helical filaments. Results have been given in the small pitch (large wavenumber) and small amplitude regime [4,11], while Ricca [11] also gives an analytic result for the infinite-torsion case, valid when the pitch is small (wavenumber is large). Additional studies on the 'cut-off' method [12] have improved on the aforementioned analytical results. In addition to results for the Biot–Savart law, note that analytical results are common under the LIA [13], which is much simpler to solve in the helical case [14,15]).

Physically, helical filaments and Kelvin waves are of fundamental importance. Numerical results and theoretical models have been used to show that a cascade of Kelvin waves transfers energy from large to small length scales [16–18], where energy is removed from the system via phonon emission [19–21]. In the case of classical fluids, Kelvin waves have been studied on thin line vortices—resulting in helical vortex filaments [22,23], and also on knotted vortex rings [24]. Regarding the quantum fluid case, Kelvin waves were observed [25] on quantized vortices after vortex reconnection events [26].

The mathematics of Kelvin waves along vortex filaments have been studied in a variety of contexts [14,15]. Van Gorder [27] studied helical vortex filaments driven by normal fluid flow in an arclength formulation of the quantum form of the LIA. Van Gorder [28] considered helical vortex filaments under the quantum LIA in which the amplitude was assumed to be a function of time, which was an improvement over Van Gorder [29] in which only constant-amplitude helices were studied in the small amplitude regime. It was shown that one can develop a mathematical model, consisting of three ordinary differential equations, which govern the temporal dynamics of the amplitude, phase and translation of the helical filaments. The case in which the amplitude is constant in time corresponds to the critical value for the Donnelly–Glaberson instability. Below this, the Kelvin waves decay, and above this the Kelvin waves amplify. Recently, Van Gorder [30] studied non-local effects under the regularized LIA for the classical helical vortex filament (in the absence of any quantum terms).

In this paper, we shall study the non-local quantum model (1.9), which incorporates both quantum and non-local effects, in order to deduce the influence of non-locality on the Kelvin wave solutions to the quantum LIA. We shall formulate the relevant model in §2, constructing a dynamical system with non-local terms that gives the dynamics of the amplitude, phase and translation of the Kelvin waves in time. In §3, we discuss asymptotic solutions in both the large and small time regimes for this model. As was true for the local model studied in Van Gorder [28], the growth or decay of the amplitude is not purely linear, with the growth or decay rate different for large or small timescales. We also obtain the Donnelly–Glaberson instability in the presence of non-locality. We demonstrate that the non-local terms have a stabilizing influence on the Kelvin waves, meaning that higher normal fluid velocities will be required to initialize amplification of Kelvin waves in the large wavenumber regime. In §4, we further consider the mathematical structure of the non-local dynamical system, enabling us to qualitatively classify the possible behaviours of these Kelvin waves. There are three distinct cases, depending on the Donnelly–Glaberson instability. There exist Kelvin waves which amplify (with the amplification rate gradually slowing in time), eternal Kelvin waves which maintain their amplitude in time (at the critical value for the Donnelly–Glaberson instability) and Kelvin waves which decay over time (with the decay rate increasing over time). We discuss all of these results in §5.

We note that this study deals with the dynamics of a single helical vortex filament. A separate, but related topic is the study of non-local Kelvin wave interactions. The latter involves the study of non-local interactions of weakly nonlinear Kelvin waves on vortex filaments. In the high wavenumber limit, Kozik & Svistunov [31] develop the Kelvin wave kinetic theory in the regime of weak turbulence, where the smallness of nonlinearities reduces the nonlinear effects to scattering processes for the harmonic modes. They find that the leading elementary process responsible for the kinetics is the three-kelvon scattering. Also, Laurie *et al*. [32] have studied the structure of the nonlinear Kelvin wave interactions, and added to the theory by including previously unaccounted leading-order contributions to the effective wave Hamiltonian governing these dynamics, and explicitly calculated the interaction coefficients. The essential role of non-locality in these types of interactions has been demonstrated [33].

2. Time evolution of Kelvin waves on a quantum vortex filament

In order to obtain the time evolution of Kelvin waves along a vortex filament, we shall study the integro-differential Cauchy problem

$$\mathbf{r}_t = \mathrm{qBS}[\mathbf{r}], \tag{2.1}$$

$$\mathbf{r}(x,0) = (x, A\cos(kx + x_0), A\sin(kx + x_0)), \tag{2.2}$$

where qBS[**r**] is the quantum Biot–Savart law with use made of the cut-off in an ϵ neighbourhood of the singularity.

From the initial profile $\mathbf{r}(x,0)$, the time evolution will involve three attributes:

(i) There will be translation of the Kelvin waves along the x-axis.
(ii) There will be rotation of the Kelvin waves orthogonal to the x-axis.
(iii) There will be decay or growth of the amplitude of the Kelvin waves, due to normal fluid and mutual friction effects.

In light of these properties, we should seek a solution of the form

$$\mathbf{r}(x,t) = (x + \beta(t), A\exp(-\mu(t))\cos(kx - \omega(t) + x_0), A\exp(-\mu(t))\sin(kx - \omega(t) + x_0)). \tag{2.3}$$

The function $\beta(t)$ governs translation along the x-axis, $\omega(t)$ governs rotations orthogonal to the x-axis, and $\mu(t)$ governs amplification or dissipation of the waves. Note that in the classical case, $\mu(t)$ is necessarily constant in time, while $\beta(t)$ and $\omega(t)$ are linear functions of time. As has been shown for the strictly local quantum model (neglecting Biot–Savart integral terms), in the presence of mutual friction and a driving normal fluid these terms are nonlinear functions of time.

We shall consider a normal fluid flow directed along the direction of the vortex filament, that is $\mathbf{U} = (U, 0, 0)$. This configuration can be used to propagate the Kelvin waves which form along the line filament. The normal fluid flow along the vortex filament line can then amplify the Kelvin waves, depending on the strength of the normal fluid velocity, U. Note that we have considered the case in which the normal fluid is uniformly directed along the vortex filament. If, instead, we were to have picked $\mathbf{U} = (U_1, U_2, U_3)$, observe that it has been shown by Shivamoggi [34] that the components orthogonal to the filament orientation (U_2 and U_3) will simply translate the entire filament structure in space. Therefore, it is the component directed along the filament which will most strongly modify the structure of the Kelvin waves.

If we place the parametric representation (2.3) into (2.1), we obtain a system of three equations. The first equation directly gives the time evolution of $\beta(t)$, while the latter two involve time derivatives of both $\omega(t)$ and $\mu(t)$. Luckily, the latter system of two equations is never degenerate, so we may solve for the time derivatives for each of $\omega(t)$ and $\mu(t)$. The full dynamics of the Kelvin waves are found to be governed by

$$\begin{aligned}\frac{\mathrm{d}\beta}{\mathrm{d}t} &= \frac{(1-\alpha')A^2k^3\exp(-2\mu(t))}{[1+A^2k^2\exp(-2\mu(t))]^{3/2}} + \frac{\alpha' UA^2k^2\exp(-2\mu(t))}{1+A^2k^2\exp(-2\mu(t))} \\ &\quad + \lambda\left\{\left(A^2k\exp(-2\mu(t)) - \frac{\alpha'A^4k^3\exp(-4\mu(t))}{1+A^2k^2\exp(-2\mu(t))}\right)J_1(\mu(t))\right. \\ &\quad \left. + \frac{\alpha'A^2k\exp(-2\mu(t))}{1+A^2k^2\exp(-2\mu(t))}J_2(\mu(t))\right\}, \end{aligned} \tag{2.4}$$

$$\begin{aligned}\frac{\mathrm{d}\omega}{\mathrm{d}t} &= \frac{(1-\alpha')k^2}{[1+A^2k^2\exp(-2\mu(t))]^{3/2}} + \frac{\alpha' Uk}{1+A^2k^2\exp(-2\mu(t))} \\ &\quad + \lambda\left\{\left(1 - \frac{\alpha'}{1+A^2k^2\exp(-2\mu(t))}\right)J_2(\mu(t)) - \frac{\alpha'A^2k^2\exp(-2\mu(t))}{1+A^2k^2\exp(-2\mu(t))}J_1(\mu(t))\right\} \end{aligned} \tag{2.5}$$

and

$$\begin{aligned}\frac{\mathrm{d}\mu}{\mathrm{d}t} &= \alpha\left\{\frac{k^2}{1+A^2k^2\exp(-2\mu(t))} - \frac{Uk}{\sqrt{1+A^2k^2\exp(-2\mu(t))}}\right\} \\ &\quad + \alpha\lambda\left\{\frac{A^2k^2\exp(-2\mu(t))}{\sqrt{1+A^2k^2\exp(-2\mu(t))}}J_1(\mu(t)) + \frac{1}{\sqrt{1+A^2k^2\exp(-2\mu(t))}}J_2(\mu(t))\right\}. \end{aligned} \tag{2.6}$$

Here, the terms $J_1(\mu(t))$ and $J_2(\mu(t))$ hold the non-local contributions,

$$J_1(\mu(t)) = \int_\epsilon^\infty \frac{1-\cos(k\sigma)}{[\sigma^2 + 2A^2\exp(-2\mu(t))\{1-\cos(k\sigma)\}]^{3/2}}\,\mathrm{d}\sigma \tag{2.7}$$

and

$$J_2(\mu(t)) = \int_\epsilon^\infty \frac{\cos(k\sigma) - 1 + k\sigma\sin(k\sigma)}{[\sigma^2 + 2A^2\exp(-2\mu(t))\{1-\cos(k\sigma)\}]^{3/2}}\,\mathrm{d}\sigma. \tag{2.8}$$

In the limit where non-local effects are negligible, we take $\lambda \to 0$, and this system reduces to that studied in Van Gorder [28]. In the limit where mutual friction effects are negligible we take $\alpha, \alpha' \to 0$, and the system reduces to that studied in Van Gorder [30]. In the limit where both non-local and mutual friction effects are negligible, we recover the classical LIA results. The dynamics here are more complicated than either of those special cases. In what follows, we shall completely determine the possible qualitative behaviours of the Kelvin waves governed under these nonlinear and non-local dynamics when the mutual friction terms are included.

3. Asymptotic solutions to the dynamical system (2.4)–(2.6)

(a) The small time limit

In the small time limit, we take $\exp(-\mu(t)) \approx 1$. Then, the response functions on the right-hand side of (2.4)–(2.6) are all independent of time. The small-time asymptotic solutions are therefore

$$\beta(t) \approx \frac{A^2k^3}{[1+A^2k^2]^{3/2}}\left(1+\lambda\frac{[1+A^2k^2]^{3/2}}{k^2}J_1(0)\right)t+\frac{\alpha' A^2k^2}{1+A^2k^2}\left(U-\frac{k}{\sqrt{1+A^2k^2}}\right)t + \frac{\alpha'\lambda A^2k}{1+A^2k^2}(J_2(0)-A^2k^2J_1(0))t \tag{3.1}$$

and

$$\omega(t) \approx \frac{k^2}{[1+A^2k^2]}(1+\lambda J_1(0))t+\frac{\alpha' k}{1+A^2k^2}\left(U-\frac{k}{\sqrt{1+A^2k^2}}\right)t-\frac{\alpha'\lambda}{1+A^2k^2}(J_2(0)+A^2k^2J_1(0))t. \tag{3.2}$$

The first term in each of these representations is the classical contribution, the second term is the localized quantum contribution, while the third term is the non-local quantum contribution. As for the decay rate, we have

$$\mu(t) \approx \frac{\alpha k}{1+A^2k^2}\left(\frac{k}{\sqrt{1+A^2k^2}}-U\right)t+\frac{\alpha\lambda}{\sqrt{1+A^2k^2}}(J_2(0)+A^2k^2J_1(0))t, \tag{3.3}$$

where the first term is the localized quantum contribution, whereas the second term is the non-local quantum contribution. (There is no classical decay, hence there is no classical decay term.) Note that the decay term scales as the negative of the quantum part of the rotation term.

In the equations above, note that the non-local terms are themselves constant in time:

$$J_1(0)=\int_\epsilon^\infty \frac{1-\cos(k\sigma)}{[\sigma^2+2A^2(1-\cos(k\sigma))]^{3/2}}\,\mathrm{d}\sigma \tag{3.4}$$

and

$$J_2(0)=\int_\epsilon^\infty \frac{\cos(k\sigma)-1+k\sigma\sin(k\sigma)}{[\sigma^2+2A^2(1-\cos(k\sigma))]^{3/2}}\,\mathrm{d}\sigma. \tag{3.5}$$

(b) Donnelly–Glaberson instability in the non-local setting

From the form of the dynamical system (2.4)–(2.6), the function $\mu(t)$ maintains its sign over time. If this function is positive, the Kelvin waves undergo decay. Meanwhile, if this function is negative, the Kelvin waves amplify over time. This latter scenario leads to instability. The critical value of the wavenumber k at which decay gives way to amplification corresponds to the Donnelly–Glaberson instability [35–37]. This instability ensures that amplification of the Kelvin waves will follow from a sufficiently large normal fluid velocity. For the strictly local case (where $\lambda = 0$), this value corresponds to

$$k_l^* = \frac{U}{\sqrt{1-A^2U^2}}. \tag{3.6}$$

At this value, the local Kelvin waves have constant amplitudes over all time. Note that this value corresponds to a steady-state solution for the dynamical system corresponding to the local model. What we shall show below is that by including the non-local terms from the Biot–Savart law, the Donnelly–Glaberson instability is modified strongly in the large wavenumber regime, while in the small wavenumber regime we essentially have the same results that are predicted in the local case.

If we consider non-local effects, we modify the value of the critical wavenumber corresponding to the Donnelly–Glaberson instability. Denote this critical wavenumber by k_n^*. Then, k_n^* must satisfy

$$\frac{k_n^*}{\sqrt{1+A^2(k_n^*)^2}}\left(\frac{k_n^*}{\sqrt{1+A^2(k_n^*)^2}}-U\right)+\lambda\int_\epsilon^\infty \frac{(A^2(k_n^*)^2-1)(1-\cos(k_n^*\sigma))+k_n^*\sigma\sin(k_n^*\sigma)}{[\sigma^2+2A^2(1-\cos(k_n^*\sigma))]^{3/2}}\,\mathrm{d}\sigma=0. \tag{3.7}$$

Solving this equation to obtain k_n^* as a function of U is not a trivial matter, even numerically. However, note that obtaining the inverse relation $U=U(k_n^*)$ is rather simple, to wit:

$$U=\frac{k_n^*}{\sqrt{1+A^2(k_n^*)^2}}+\lambda\frac{\sqrt{1+A^2(k_n^*)^2}}{k_n^*}\int_\epsilon^\infty \frac{(A^2(k_n^*)^2-1)(1-\cos(k_n^*\sigma))+k_n^*\sigma\sin(k_n^*\sigma)}{[\sigma^2+2A^2(1-\cos(k_n^*\sigma))]^{3/2}}\,\mathrm{d}\sigma. \tag{3.8}$$

For comparison, in the strictly local case, we will have

$$U=\frac{k_l^*}{\sqrt{1+A^2(k_l^*)^2}}. \tag{3.9}$$

For small k_n^*, the integral term in (3.8) is negative, while for large k_n^*, the integral term in (3.8) is positive. There will exist some intermediate value of k_n^* for which the integral term is exactly zero, in which case $k_n^*=k_l^*$. This value will correspond to some specific value of U, say U^*, and we define U^* as the unique value at which $k_n^*(U^*)=k_l^*(U^*)$. For $U<U^*$, we have $k_n^*(U)<k_l^*(U)$, hence for small normal fluid velocities the inclusion of non-local effects decreases the critical wavenumber at which we observe the Donnelly–Glaberson instability. On the other hand, $U>U^*$, we have $k_n^*(U)>k_l^*(U)$, so for large values of the normal fluid velocity, the non-local effects increase the critical wavenumber at which we observe the Donnelly–Glaberson instability.

Note also that in the local model, the value of the normal fluid velocity is bounded like $U<1/A$. However, as we see here, this is due strictly to the locality of the problem. For the non-local problem, there is no such bound on the normal fluid velocity. This means that the non-local terms are having a smoothing effect, and hence large normal fluid velocity values are permitted as they do not result in a blowup of the critical wavenumber. Physically, this means that for any $U>1/A$, the local model implies that all solutions amplify. However, including non-local contributions, we see that solutions in the presence of large normal fluid velocity can decay, provided that we have large wavenumbers. In figure 1, we plot stability regions obtained by both the local and non-local models. It is clear that the non-locality has a smoothing effect, resulting in decaying Kelvin waves in the large wavenumber regime where the local theory would predict amplification.

These results suggest that higher normal fluid velocity values will be required to initialize amplification of Kelvin waves, when wavenumbers are high (i.e. when then helix is tightly coiled). In the large wavenumber regime, the non-locality therefore has a smoothing or stabilizing effect on the Kelvin waves. Part of the reason for the discrepancy lies in the fact that the LIA poorly approximates tightly coiled vortex filaments, and for such filaments the full Biot–Savart dynamics are required. This stability result therefore points to the qualitative breakdown of the LIA for helical vortex filaments in the large wavenumber regime.

(c) The large time limit

In the very large time limit, we have either $\exp(-\mu(t))\to 0$ if there is decay of the Kelvin waves, or $\exp(-\mu(t))\to\infty$ if there is amplification of the Kelvin waves.

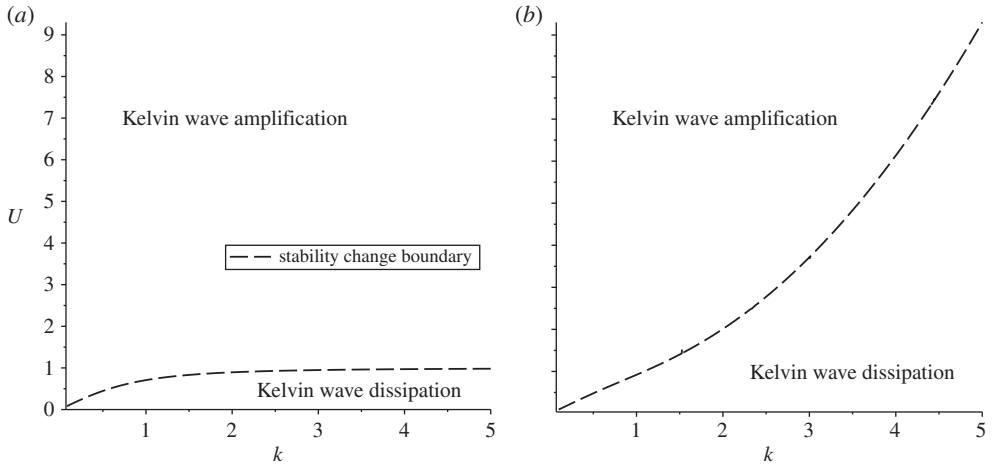

Figure 1. Plot of the stability curve and amplification/de-amplification regimes for Kelvin waves in the k-U plane under the local model (*a*) and the non-local model (*b*). For the local model, we set $\lambda = 0$ and obtain the quantum LIA. For the non-local model, we set $\epsilon = 10^{-3}$ and hence $\lambda = 1/3\ln(10)$. For each plot, we have used $\alpha = 0.006$, $\alpha' = 0.003$, $A = 1$.

In the case of Kelvin wave decay, the solutions should behave in large timescales like

$$\beta(t) \approx \beta_\infty, \tag{3.10}$$

$$\omega(t) \approx \{(1-\alpha')(k^2 + \lambda J_2(\infty)) + \alpha' kU\}t + \omega_\infty \tag{3.11}$$

and

$$\mu(t) \approx \alpha\{k(k-U) + \lambda J_2(\infty)\}t + \mu_\infty. \tag{3.12}$$

Here, β_∞, ω_∞ and μ_∞ are all constants and $J_2(\infty)$ is given by

$$\begin{aligned} J_2(\infty) &= \int_\epsilon^\infty \frac{\cos(k\sigma) - 1 + k\sigma\sin(k\sigma)}{\sigma^3}\,\mathrm{d}\sigma \\ &= \frac{k^2}{2}\mathrm{Ci}(k\epsilon) + \frac{1 - \cos(k\epsilon) - k\epsilon\sin(k\epsilon)}{2\epsilon^2} \\ &= \frac{2\gamma - 1}{4}k^2 + \frac{k^2}{2}\ln(k\epsilon) + O(\epsilon^2). \end{aligned} \tag{3.13}$$

On the other hand, in the case of Kelvin wave amplification, the solutions should behave in large timescales rather differently. This is due to the fact that, when $\exp(-\mu(t)) \to 0$, the nonlinear response functions are linearized and one can perform the requisite integrations, obtaining linear functions. So, in the case of decaying Kelvin waves, linear approximations to the solutions are reasonable at small and large timescales. However, when $\exp(-\mu(t)) \to \infty$, the time derivative of $\mu(t)$ tends to zero. So, the function $\mu(t)$ should decrease more slowly than a linear function. If we balance the dominant terms and seek a solution which tends more slowly to infinity than a linear function, we find that the growth rate function scales like

$$\mu(t) \approx -\ln\left(\frac{\alpha U}{A}t + n_0\right), \tag{3.14}$$

where n_0 is a constant. Interestingly, while the decay of a Kelvin wave is of the order of an exponential rate of decay, the amplification of a Kelvin wave is at a much more gradual logarithmic rate.

The rotational velocity should then scale like

$$\frac{\mathrm{d}\omega}{\mathrm{d}t} \approx \frac{k^2 + \lambda J_2(\infty)}{[1 + A^2k^2\exp(-2\mu(t))]^{3/2}} - \frac{\alpha'}{\alpha}\frac{1}{\sqrt{1 + A^2k^2\exp(-2\mu(t))}}\frac{\mathrm{d}\mu}{\mathrm{d}t}$$
$$\approx \frac{k^2 + \lambda J_2(\infty)}{[1 + \alpha^2U^2k^2t^2]^{3/2}} + \frac{\alpha'}{\alpha}\frac{1}{t\sqrt{1 + \alpha^2U^2k^2t^2}}, \tag{3.15}$$

hence

$$\omega(t) \approx \frac{(k^2 + \lambda J_2(\infty))t}{\sqrt{1 + \alpha^2U^2k^2t^2}} - \frac{\alpha'}{\alpha}\tanh^{-1}\left(\frac{1}{\sqrt{1 + \alpha^2U^2k^2t^2}}\right). \tag{3.16}$$

The first (classical) term is positive, increasing and remains bounded, whereas the quantum contribution is negative, increasing and bounded for large timescales. In fact, we have that for $\alpha > 0$,

$$\omega(t) = \frac{k^2 + \lambda J_2(\infty)}{\alpha Uk} + O\left(\frac{1}{t}\right) \tag{3.17}$$

as t becomes large. This means that the phase term tends towards a constant, and thus there is no rotational motion, for large time. Meanwhile, if $\alpha \to 0$, then we recover the classical limit

$$\omega(t) \approx (k^2 + \lambda J_2(\infty))t. \tag{3.18}$$

In this limit, the rotational velocity remains constant in time. Therefore, in the presence of quantum effects, the amplifying Kelvin waves rotate progressively slower as they increasingly amplify, at large timescales.

The term J_1 is the non-local correction to the translational velocity, $\mathrm{d}\beta/\mathrm{d}t$, while J_2 is the non-local correction to the rotational velocity, $\mathrm{d}\omega/\mathrm{d}t$, in the absence of mutual friction effects. As seen above, these terms make additional appearances when there are mutual friction effects. Now, in the large time limit, the translational velocity tends to zero, hence terms with J_1 tend to zero, while the rotational velocity is non-zero, so we still have a contribution from J_2 at large times.

Plots of the small and large time asymptotics for the decay or growth term, $\mu(t)$, are provided in figure 2 along with corresponding numerical solutions. This demonstrates the accuracy of the asymptotic expressions given above. As the dynamics of $\beta(t)$ and $\omega(t)$ are determined from $\mu(t)$, the asymptotics for these functions are also accurate, where valid.

Note that we do not discuss the possibility of self-reconnections that can completely change the structure of the vortex filament [38]. This is because our Kelvin wave model consists of a single helical vortex filament, and there is no mechanism for this to break and then reconnect. However, if the Kelvin wave amplitude is significantly large compared with its period, then the prospect of self-reconnection would be possible. Therefore, in the case of Kelvin wave amplification, one can

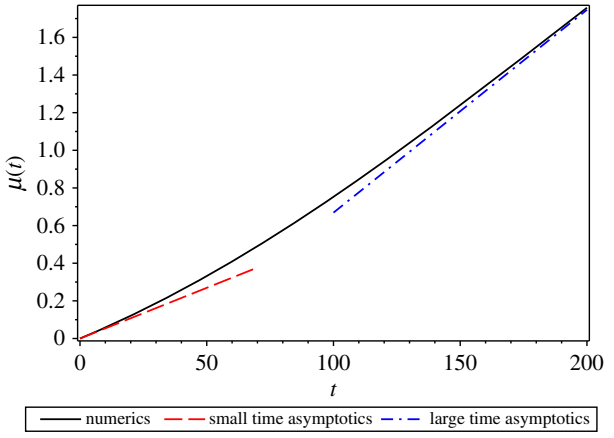

Figure 2. Plot of the decay rate $\mu(t)$ when we set $\epsilon = 10^{-3}$ and hence $\lambda = 1/3\ln(10)$. The physical parameters are $k = 1.5$, $U = 1, \alpha = 0.006, \alpha' = 0.003, A = 0.5$. We see that the small time asymptotics are indeed rather accurate for small enough t, while the large time asymptotics are accurate for large t. Importantly, this demonstrates that the decay rate does scales as a linear function in both the small and large timescales. However, the rate of decay differs in each timescales, with the decay more rapid at large timescales. (Online version in colour.)

view the large time dynamics as governing the structure of the vortex filament up until the point before any self-reconnections may take place. Of course, there must be some breakdown of the structure before the Kelvin wave amplitude becomes very large.

4. Dynamics of the system (2.4)–(2.6)

Note from the form of the system (2.4)–(2.6) that if we understand the dynamics of $\mu(t)$, we immediately can determine the dynamics of $\beta(t)$ and $\omega(t)$. Still, (2.6) is rather complicated. To better study this equation, let us make the transformation

$$\theta(t) = \frac{1}{\sqrt{1 + A^2k^2\exp(-2\mu(t))}}. \tag{4.1}$$

Under an appropriate change of variable ($\chi = k\sigma$), we can then write the integrals $J_1(\mu(t))$ and $J_2(\mu(t))$ as

$$J_1(\mu(t)) = k^2\int_{k\epsilon}^{\infty} \frac{1-\cos(\chi)}{[\chi^2 + 2(1-\cos(\chi))(\theta^{-2}(t)-1)]^{3/2}}\,\mathrm{d}\chi \tag{4.2}$$

and

$$J_2(\mu(t)) = k^2\int_{k\epsilon}^{\infty} \frac{\cos(\chi) - 1 + \chi\sin(\chi)}{[\chi^2 + 2(1-\cos(\chi))(\theta^{-2}(t)-1)]^{3/2}}\,\mathrm{d}\chi. \tag{4.3}$$

Under the transformation (4.1), equation (2.6) becomes

$$\frac{\mathrm{d}\theta}{\mathrm{d}t} = \alpha k^2(1-\theta^2)\theta^2\left(\theta - \frac{U}{k}\right) + \alpha k^2\lambda(1-\theta^2)\int_{k\epsilon}^{\infty} \frac{(1-2\theta^2)(1-\cos(\chi)) + \theta^2\chi\sin(\chi)}{[\chi^2 + 2(1-\cos(\chi))(\theta^{-2}-1)]^{3/2}}\,\mathrm{d}\chi. \tag{4.4}$$

From the transform (4.1), the appropriate initial condition is $\theta(0) = (1 + A^2k^2)^{-1/2}$. Furthermore, as $\mu(t)$ is assumed to be a real-valued function, we must have $0 < \theta(t) < 1$ for all finite t. If $\theta \to 0^+$, then $\mu \to -\infty$ and the Kelvin waves amplify. Meanwhile, if $\theta \to 1^-$, then $\mu \to \infty$ and the Kelvin waves decay.

Equation (4.4) has equilibrium points $\theta_1^* = 0$, $\theta_2^* = (1 + A^2(k_n^*(U))^2)^{-1/2}$ and $\theta_3^* = 1$, with $\theta_1^* < \theta_2^* < \theta_3^*$. One may show that θ_1^* and θ_3^* are stable, while θ_2^* is unstable. As the equation is first order and autonomous, there are no non-equilibrium dynamics for large time. Therefore, the dynamics of (4.4) can be described qualitatively as follows:

(i) If $\theta_2^* < \theta(0) < \theta_3^*$, then $\theta \to 1^-$ for large t. This implies that $\mu \to \infty$, and hence the Kelvin waves decay over time.
(ii) If $\theta(0) = \theta_2^*$, then $\theta(t) \equiv \theta_2^*$ for all t. This implies that $\mu(t)$ is constant, and hence that the Kelvin waves maintain a constant amplitude for all time. This corresponds to the classical helical filament without dissipation.
(iii) If $\theta_1^* < \theta(0) < \theta_2^*$, then $\theta \to 0^+$ for large t. This implies that $\mu \to -\infty$, and hence the Kelvin waves amplify over time.

The value of the equilibrium θ_2^* of course depends on U. However, as for each value of $U \geq 0$, a critical wavenumber $k_n^*(U)$ exists (as per our discussion in §3), the properties above are true even for large normal fluid velocities. This is in contrast to the localized model, given by

$$\frac{\mathrm{d}\theta}{\mathrm{d}t} = \alpha k^2 (1-\theta^2)\theta^2 \left(\theta - \frac{U}{k}\right). \tag{4.5}$$

For this model, such an equilibrium exists for small enough U (in particular, for $U < 1/A$) while for larger U the equilibrium value would exceed one. In such a scenario, the zero equilibrium would be attractive while the equilibrium equal to one would be repulsive. A larger equilibrium, $\theta_4^* = U/k > 1$, would be attractive yet non-physical as $\theta > 1$ implies that μ is not real-valued. In such a case, all solutions $0 < \theta(t) < 1$ would tend to zero and imply the amplification of Kelvin waves over time. This is exactly what the asymptotics of the previous section suggested.

Note that the dynamics of $\theta(t)$ (and hence of $\mu(t)$) are 'slow' for intermediate wave numbers, in that they scale with αk^2. Therefore, the dynamics described above are order $O(\alpha)$. In the very cold limit where $\alpha \to 0$, these dynamics become negligible, whereas in the warmer superfluid limit these dynamics become stronger (as $\alpha = O(1)$ in the warm superfluid limit above 2.0K). However, the dynamics for $\beta(t)$ and $\omega(t)$ are always of order $O(1)$. This makes sense, as both translational and rotational effects are present in the classical limit, whereas the amplification or decay of Kelvin waves in this model is a purely quantum effect.

(a) Approximate dynamics

We may approximate the differential equation (4.4) in order to better understand the nonlinear dynamical process under which Kelvin waves decay or amplify. In particular, note that the approximation

$$\frac{1}{[\chi^2 + a(1-\cos(\chi))]^{3/2}} \approx \frac{1}{\chi^3 (1+a/2)^{3/2}} \tag{4.6}$$

is rather accurate for both small and large χ. Using this approximation, we have

$$\begin{aligned}
&\int_{k\epsilon}^{\infty} \frac{(1-2\theta^2)(1-\cos(\chi)) + \theta^2 \chi \sin(\chi)}{[\chi^2 + 2(1-\cos(\chi))(\theta^{-2}-1)]^{3/2}}\,\mathrm{d}\chi \\
&\quad = \frac{1}{[1+(\theta^{-2}-1)]^{3/2}} \int_{k\epsilon}^{\infty} \frac{(1-2\theta^2)(1-\cos(\chi)) + \theta^2 \chi \sin(\chi)}{\chi^3}\,\mathrm{d}\chi \\
&\quad = \theta^3 \{a_1(k\epsilon)\theta^2 + a_2(k\epsilon)\},
\end{aligned} \tag{4.7}$$

where

$$a_1(k\epsilon) = \frac{\cos(k\epsilon) - 1}{(k\epsilon)^2} = -\frac{1}{2} + O((k\epsilon)^2) \tag{4.8}$$

and

$$\begin{aligned}
a_2(k\epsilon) &= \frac{1}{2}\left\{\frac{k\epsilon \sin(k\epsilon) + 1 - \cos(k\epsilon)}{(k\epsilon)^2} - \mathrm{Ci}(k\epsilon)\right\} \\
&= \frac{3-2\gamma}{4} - \frac{1}{2}\ln(k\epsilon) + O((k\epsilon)^2).
\end{aligned} \tag{4.9}$$

Under this approximation, equation (4.4) reduces to a polynomial differential equation

$$\frac{\mathrm{d}\theta}{\mathrm{d}t} = \alpha k^2\theta^2(1-\theta^2)\left\{\frac{a_1(k\epsilon)}{\ln(\epsilon^{-1})}\theta^3 + \left(1+\frac{a_2(k\epsilon)}{\ln(\epsilon^{-1})}\right)\theta - \frac{U}{k}\right\}. \tag{4.10}$$

Compared with the equation arising from the local model, (4.5), equation (4.10) has a higher-order polynomial term. Provided k is not too large, this term suggests the existence of an equilibrium value between zero and one even if U is larger than $1/A$. (If k is very large, the approximation of the integral breaks down as the term $k\epsilon$ may no longer be small.) The dynamics of equation (4.10) agree nicely with those of the more complicated equation (4.4) which involves an integral term, suggesting that equation (4.4) behaves essentially like the polynomial differential equation (4.10).

(b) Recovery of the vortex filament parameters

As we now understand the qualitative dynamics of the system (4.4), we use this to study the dynamics of the system (2.4)–(2.6). First, note that we immediately obtain (from equation (4.1))

$$\mu(t) = \ln\left(\frac{Ak\theta(t)}{\sqrt{1-\theta^2(t)}}\right). \tag{4.11}$$

Clearly, if $\theta \to 0$ then $\mu \to -\infty$, and the Kelvin waves amplify in time. Conversely, if $\theta \to 1$ then $\mu \to \infty$, and the Kelvin waves decay in time. As $\theta(t)$ is always monotone in time, then so is $\mu(t)$.

In order to recover the phase term, $\omega(t)$, note that we may write (2.5) in the form

$$\frac{\mathrm{d}\omega}{\mathrm{d}t} = \frac{k^2}{[1+A^2k^2\exp(-2\mu(t))]^{3/2}} + \lambda J_2(\mu(t)) - \frac{\alpha'}{\alpha}\frac{1}{\sqrt{1+A^2k^2\exp(-2\mu(t))}}\frac{\mathrm{d}\mu}{\mathrm{d}t}. \tag{4.12}$$

Integrating, we obtain

$$\begin{aligned}\omega(t) &= \int_0^t \left\{\frac{k^2}{[1+A^2k^2\exp(-2\mu(\tau))]^{3/2}} + \lambda J_2(\mu(\tau))\right\}\mathrm{d}\tau - \frac{\alpha'}{\alpha}\ln\left(\frac{\exp(\mu(t)) + \sqrt{\exp(2\mu(t)) + A^2k^2}}{1+\sqrt{1+A^2k^2}}\right)\\ &= \int_0^t \left\{k^2\theta(\tau)^3 + \lambda k^2\int_{k\epsilon}^{\infty}\frac{\cos(\chi)-1+\chi\sin(\chi)}{[\chi^2+2(1-\cos(\chi))(\theta(\tau)^{-2}-1)]^{3/2}}\,\mathrm{d}\chi\right\}\mathrm{d}\tau\\ &\quad - \frac{\alpha'}{\alpha}\ln\left(\frac{Ak}{1+\sqrt{1+A^2k^2}}\sqrt{\frac{1+\theta(t)}{1-\theta(t)}}\right).\end{aligned} \tag{4.13}$$

The first term is the direct analogue of the non-local result in Van Gorder [30] for the classical case. The difference between this term and the purely classical case is that the time dependence of $\mu(t)$ means that this term is not simply a linear function of time. Aside from this, the terms look nearly the same. The second term is the quantum effect due to dissipation or amplification of the Kelvin waves. While both α and α' are in general small parameters for the cold superfluid case, the ratio is often $\alpha'/\alpha = O(1)$. So, the term giving the quantum correction is not particularly small. Approximating the non-local contribution as above, we obtain

$$\omega(t) \approx (k^2 + \lambda J_2(\infty))\int_0^t \theta(\tau)^3\,\mathrm{d}\tau - \frac{\alpha'}{\alpha}\ln\left(\frac{Ak}{1+\sqrt{1+A^2k^2}}\sqrt{\frac{1+\theta(t)}{1-\theta(t)}}\right). \tag{4.14}$$

To recover the translation term, $\beta(t)$, we may write (2.4) as

$$\begin{aligned}\frac{\mathrm{d}\beta}{\mathrm{d}t} &= A^2k\exp(-2\mu(t))\left\{\frac{k^2}{[1+A^2k^2\exp(-2\mu(t))]^{3/2}} + \lambda J_1(\mu(t))\right\}\\ &\quad - \frac{\alpha'}{\alpha}\frac{A^2k\exp(-2\mu(t))}{\sqrt{1+A^2k^2\exp(-2\mu(t))}}\frac{\mathrm{d}\mu}{\mathrm{d}t} + \frac{2\alpha'\lambda A^2k\exp(-2\mu(t))}{1+A^2k^2\exp(-2\mu(t))}J_2(\mu(t)).\end{aligned} \tag{4.15}$$

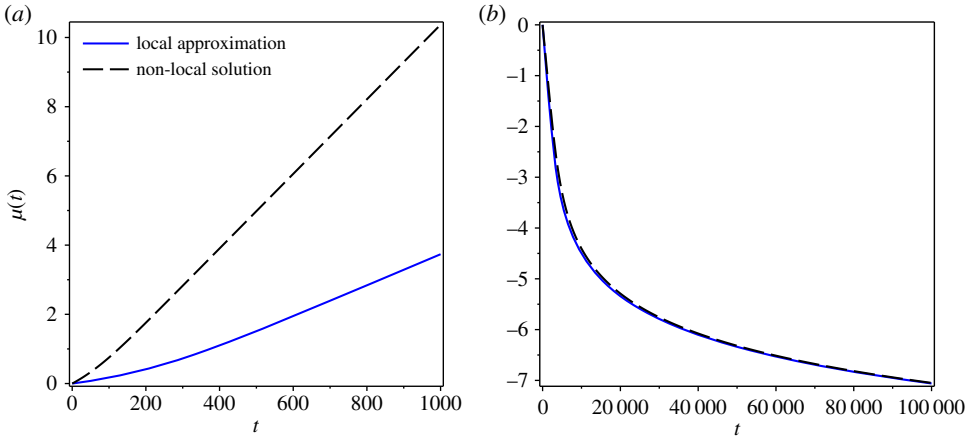

Figure 3. Plot of the function $\mu(t)$ when there is (*a*) decay of Kelvin waves or (*b*) amplification of Kelvin waves. In each plot, we provide the solution including only local effects ($\lambda = 0$), and a solution including non-local effects. In the latter case, we set $\epsilon = 10^{-3}$ and hence $\lambda = 1/3\ln(10)$. For (*a*), we take $k = 1.5$ (so that the Kelvin waves decay) and for (*b*) we take $k = 0.2$ (so that the Kelvin waves amplify). The remaining physical parameters used are $U = 1$, $\alpha = 0.006$, $\alpha' = 0.003$, $A = 0.5$. Initial conditions are taken as $\beta(0) = \omega(0) = \mu(0) = 0$. (Online version in colour.)

Integrating this equation, we have

$$\frac{\mathrm{d}\beta}{\mathrm{d}t} = A^2k\int_0^t \left\{ \frac{k^2}{[1+A^2k^2\exp(-2\mu(\tau))]^{3/2}} + \lambda J_1(\mu(\tau)) \right\} \exp(-2\mu(\tau))\,\mathrm{d}\tau + \frac{\alpha'}{\alpha k}\left(\sqrt{1+A^2k^2\exp(-2\mu(t))} - \sqrt{1+A^2k^2}\right) + 2\alpha'\lambda A^2k\int_0^t \frac{\exp(-2\mu(\tau))J_2(\mu(\tau))}{1+A^2k^2\exp(-2\mu(\tau))}\,\mathrm{d}\tau. \quad (4.16)$$

The first term is again the direct analogue of what we have previously seen in the classical case Van Gorder [30], with the exception being that now we have an integral over a time-dependent function $\mu(t)$ and hence the first term is not a linear function of time. Other than this, the leading term is exactly what we have seen before in the non-local classical case. The second term is not necessarily small, as again $\alpha'/\alpha = O(1)$. This term is due to the amplification or decay of the Kelvin wave. If the Kelvin wave amplifies, this term is positive, and hence this term increases the translational rate of the wave. On the other hand, when there is decay of the Kelvin wave, this term decreases the translational rate of propagation. The final term is an additional non-local term which also depends on the mutual friction parameter α', and hence this term is small. One can view this term as a non-local correction to the $O(1)$ mutual friction term modifying propagation of the Kelvin waves along the line filament.

In figures 3–5, we give numerical solutions for the decay term $\mu(t)$, the translation term $\beta(t)$, and the phase term $\omega(t)$ for both the local ($\lambda = 0$) and non-local ($\lambda > 0$) models. We consider two cases, one in which there is decay and one in which there is amplification of the Kelvin waves.

First, consider the cases in which the Kelvin waves decay. When non-local terms are included, the decay rate is increased (as non-locality smooths the dynamics). As the translational propagation of these waves is strongly tied to their decay rate, the waves in the non-local model exhibit less translational motion (and hence lower translational velocity) before translational effects become null. Recall that translation stops when the waves have decayed. On the other hand, rotational velocity is seen to be higher in the presence of non-local terms. Hence, the more natural inclusion of non-local effects results in increased rotation and decreased translation of the Kelvin waves. These Kelvin waves decay more rapidly than do their counterparts from the local model.

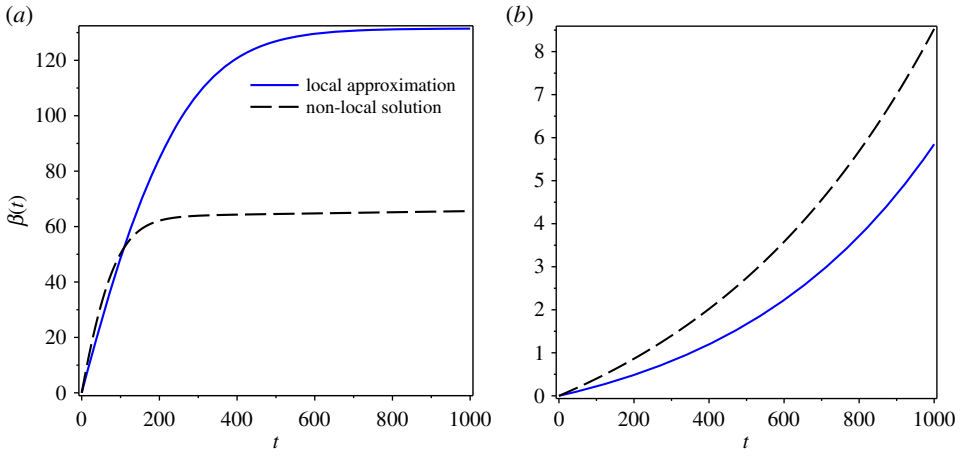

Figure 4. Plot of the function $\beta(t)$ when there is (*a*) decay of Kelvin waves or (*b*) amplification of Kelvin waves. In each plot, we provide the solution including only local effects ($\lambda = 0$), and a solution including non-local effects. In the latter case, we set $\epsilon = 10^{-3}$ and hence $\lambda = 1/3\ \ln(10)$. For (a), we take $k = 1.5$ (so that the Kelvin waves decay) and for (b) we take $k = 0.2$ (so that the Kelvin waves amplify). The remaining physical parameters used are $U = 1$, $\alpha = 0.006$, $\alpha' = 0.003$, $A = 0.5$. Initial conditions are taken as $\beta(0) = \omega(0) = \mu(0) = 0$. (Online version in colour.)

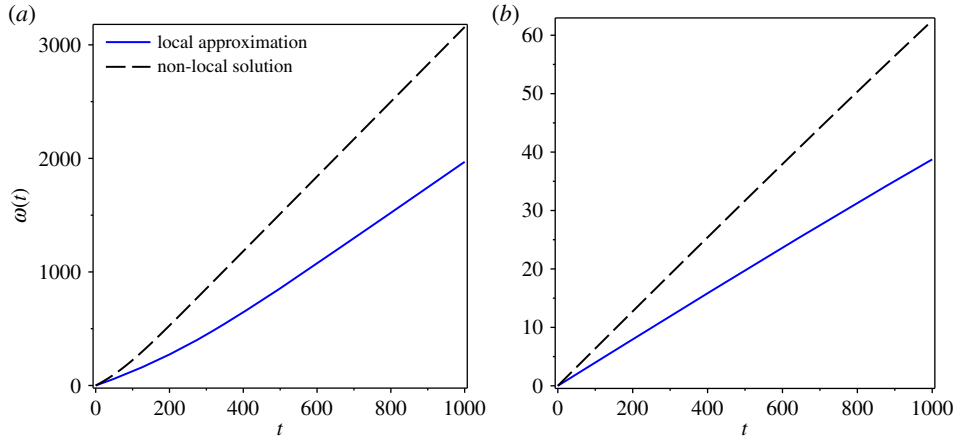

Figure 5. Plot of the function $\omega(t)$ when there is (*a*) decay of Kelvin waves or (*b*) amplification of Kelvin waves. In each plot, we provide the solution including only local effects ($\lambda = 0$), and a solution including non-local effects. In the latter case, we set $\epsilon = 10^{-3}$ and hence $\lambda = 1/3\ \ln(10)$. For (*a*), we take $k = 1.5$ (so that the Kelvin waves decay) and for (*b*) we take $k = 0.2$ (so that the Kelvin waves amplify). The remaining physical parameters used are $U = 1$, $\alpha = 0.006$, $\alpha' = 0.003$, $A = 0.5$. Initial conditions are taken as $\beta(0) = \omega(0) = \mu(0) = 0$. (Online version in colour.)

In the case where Kelvin waves amplify, we observe that $\mu(t)$ scales as a logarithmic rather than a linear function, which is exactly what the asymptotics predicted. The amplification rate is slightly higher for the Kelvin waves obtained from the local model, although the difference between the two is less evident than before due to the small differences visible in the logarithmic functions. (By contrast, larger differences are evident in the case of decay, as the function $\mu(t)$ scales as a linear function in that case.) The rotational velocity is still greater in the non-local case, in the presence of Kelvin wave amplification. However, the translational motion is greater in the non-local case, which is the reverse of what was observed in the Kelvin wave decay regime.

The general behaviour of solutions with respect to changes in the mutual friction or normal fluid velocity are in qualitative agreement with the purely local dynamical model of Van

Gorder [28]. Therefore, the primary influence of the non-locality in the present model is to modify the growth or decay of the Kelvin waves, as evidenced from the modification to the Donnelly–Glaberson stability boundary.

5. Discussion

We have reduced the non-local form of the Schwarz model (with regularized Biot–Savart integral for which the core region is approximated via LIA) to a system of three nonlinear integro-differential equations governing the temporal dynamics of Kelvin waves along a vortex filament. The model governs the amplitude and phase of the Kelvin waves, as well as their translational motion along the vortex filament. Through an analytical and numerical analysis of the governing dynamical system, we have been able to classify the possible behaviour of Kelvin waves propagating along vortex filaments in the non-local form of the Schwarz model. The primary difference between the possible Kelvin waves is whether they amplify, remain of fixed amplitude, or decay, and it is shown that the non-locality of the studied model strongly influences the boundary separating these three behaviours, particularly for Kelvin waves of large wavenumber.

These results suggest that the non-local terms have a very strong moderating effect on the Donnelly–Glaberson instability, in the case where the wavenumber is large. Therefore, it would take a far larger normal fluid velocity directed along the vortex filament in order to experimentally induce amplification of Kelvin waves. The effect is present when mutual friction is very small (temperatures near 0 K) or even of order unity (temperatures near 2 K). This highlights the fact that the LIA, while very useful in some regimes, is not valid when the vortex filaments are of large variation. In the large wavenumber regime, the helical filament becomes tightly coiled, and non-local effects due to the Biot–Savart law are poorly approximated under the LIA. Contrast this to the small wavenumber case, where the helical filaments are very loosely coiled, and the Donnelly–Glaberson instability boundary for the local and non-local case is in qualitative agreement.

We see that the primary role of the mutual friction parameter α is to modify the rate of amplification or decay of the Kelvin waves. In the low-temperature limit, this parameter is very small, and any amplification or decay of Kelvin waves will be gradual. On the other hand, when the temperature is on the order 2 K, α is of order unity, and the amplification or decay of Kelvin waves will be much more rapid. Therefore, the very low-temperature limit (say, below 1.5 K) is best for observing any nuanced growth or decay of these waves experimentally.

The analytical, and in particular, asymptotic solutions to the non-local dynamical system demonstrate that the rates of decay or amplification of the Kelvin waves are not constant over time. Rather, in the case of decay, the rate of decay starts out more gradually, and then intensifies as the Kelvin wave dies. On the other hand, in the regime in which Kelvin waves amplify, we see that the rate of growth is highest at the onset of amplification, and then the Kelvin waves grow more slowly for large time. The constant amplitude Kelvin waves are a very special case, existing along the instability boundary, and a perturbation of these solutions will result in amplification or decay (depending on the direction of the perturbation). While it is interesting to note that the constant amplitude solutions are a special case in the quantum model, recall that they are the only solution in the classical model (as amplification or decay is only possible due to the added quantum terms).

Data accessibility. This work has no data.
Competing interests. I have no competing interests.
Funding. The author received no funding for this work.

References

1. Da Rios LS. 1906 Sul moto d'un liquido indefinite con un filetto vorticoso di forma qualunque. *Rend. Circ. Mat. Palermo* **22**, 117–135 (doi:10.1007/BF03018608)

2. Arms RJ, Hama FR. 1965 Localized-induction concept on a curved vortex and motion of an elliptic vortex ring. *Phys. Fluids* **8**, 553. (doi:10.1063/1.1761268)
3. Ricca RL. 1991 Rediscovery of Da Rios equations. *Nature* **352**, 561–562 (doi:10.1038/352561a0)
4. Widnall SE. 1972 The stability of a helical vortex filament. *J. Fluid Mech.* **54**, 641–663 (doi:10.1017/S0022112072000928)
5. Boffetta G, Celani A, Dezzani D, Laurie J, Nazarenko S. 2009 Modeling Kelvin wave cascades in superfluid helium. *J. Low Temp. Phys.* **156**, 193–214 (doi:10.1007/s10909-009-9895-x)
6. Schwarz KW. 1985 Three-dimensional vortex dynamics in superfluid ^{4}He: line–line and line–boundary interactions. *Phys. Rev. B* **31**, 5782. (doi:10.1103/PhysRevB.31.5782)
7. Hall HE, Vinen WF. 1956 The rotation of liquid helium II. I. Experiments on the propagation of second sound in uniformly rotating helium II. *Proc. R. Soc. Lond. A* **238**, 204–214. (doi:10.1098/rspa.1956.0214)
8. Hall HE, Vinen WF. 1956 The rotation of liquid helium II. II. The theory of mutual friction in uniformly rotating helium II. *Proc. R. Soc. Lond. A* **238**, 215–234 (doi:10.1098/rspa.1956.0215)
9. Moore DW, Saffman PG. 1972 The motion of a vortex filament with axial flow. *Phil. Trans. R. Soc. Lond. A* **272**, 403–429 (doi:10.1098/rsta.1972.0055)
10. Saffman PG. 1992 *Vortex dynamics*. Cambridge, UK: Cambridge University Press.
11. Ricca RL. 1994 The effect of torsion on the motion of a helical vortex filament. *J. Fluid Mech.* **273**, 241–259 (doi:10.1017/S0022112094001928)
12. Boersma J, Wood DH. 1999 On the self-induced motion of a helical vortex. *J. Fluid Mech.* **384**, 263–279 (doi:10.1017/S002211209900422X)
13. Zhou H. 1997 On the motion of slender vortex filaments. *Phys. Fluids* **9**, 970–981. (doi:10.1063/1.869192)
14. Kida S. 1981 A vortex filament moving without change of form. *J. Fluid Mech.* **112**, 397–409 (doi:10.1017/S0022112081000475)
15. Sonin EB. 2012 Dynamics of helical vortices and helical-vortex rings. *EPL* **97**, 46002. (doi:10.1209/0295-5075/97/46002)
16. Kivotides D, Vassilicos JC, Samuels DC, Barenghi CF. 2001 Kelvin waves cascade in superfluid turbulence. *Phys. Rev. Lett.* **86**, 3080–3083. (doi:10.1103/PhysRevLett.86.3080)
17. L'vov V, Nazarenko S, Rudenko O. 2007 Bottleneck crossover between classical and quantum superfluid turbulence. *Phys. Rev. B* **76**, 024520. (doi:10.1103/PhysRevB.76.024520)
18. Kozik EV, Svistunov BV. 2009 Theory of decay of superfluid turbulence in the low-temperature limit. *J. Low Temp. Phys.* **156**, 215–267. (doi:10.1007/s10909-009-9914-y)
19. Nore C, Abid M, Brachet M. 1997 Kolmogorov turbulence in low-temperature superflows. *Phys. Rev. Lett.* **78**, 3896–3899. (doi:10.1103/PhysRevLett.78.3896)
20. Leadbeater M, Winiecki T, Samuels DC, Barenghi CF, Adams CS. 2001 Sound emission due to superfluid vortex reconnections. *Phys. Rev. Lett.* **86**, 1410–1413. (doi:10.1103/PhysRevLett.86.1410)
21. Vinen WF, Tsubota M, Mitani A. 2003 Kelvin-wave cascade on a vortex in superfluid 4He at a very low temperature. *Phys. Rev. Lett.* **91**, 135301. (doi:10.1103/PhysRevLett.91.135301)
22. Hopfinger EJ, Browand FK. 1982 Vortex solitary waves in a rotating, turbulent flow. *Nature* **295**, 393–395. (doi:10.1038/295393a0)
23. Maxworthy T, Hopfinger EJ, Redekopp LG. 1985 Wave motions on vortex cores. *J. Fluid Mech.* **151**, 141–165. (doi:10.1017/S0022112085000908)
24. Kleckner D, Irvine WTM. 2013 Creation and dynamics of knotted vortices. *Nat. Phys.* **9**, 253–258. (doi:10.1038/nphys2560)
25. Fonda E, Meichle DP, Ouellette NT, Hormoz S, Lathrop DP. 2014 Direct observation of Kelvin waves excited by quantized vortex reconnection. *Proc. Natl Acad. Sci. USA* **111**, 4707–4710 (doi:10.1073/pnas.1312536110)
26. Kursa M, Bajer K, Lipniacki T. 2011 Cascade of vortex loops initiated by a single reconnection of quantum vortices. *Phys. Rev. B* **83**, 014515. (doi:10.1103/PhysRevB.83.014515)
27. Van Gorder RA. 2014 Quantum vortex dynamics under the tangent representation of the local induction approximation. *J. Fluid Mech.* **740**, 5–16 (doi:10.1017/jfm.2013.626)
28. Van Gorder RA. 2014 Decay of helical Kelvin waves on a quantum vortex filament. *Phys. Fluids* **26**, 075101. (doi:10.1063/1.4887519)
29. Van Gorder RA. 2013 Motion of a helical vortex filament in superfluid 4He under the extrinsic form of the local induction approximation. *Phys. Fluids* **25**, 085101. (doi:10.1063/1.4816639)
30. Van Gorder RA. 2015 Helical vortex filament motion under the non-local Biot–Savart model. *J. Fluid Mech.* **762**, 141–155 (doi:10.1017/jfm.2014.639)

31. Kozik E, Svistunov B. 2004 Kelvin-Wave cascade and decay of superfluid turbulence. *Phys. Rev. Lett.* **92**, 035301. (doi:10.1103/PhysRevLett.92.035301)
32. Laurie J, L'vov V, Nazarenko S, Rudenko O. 2010 Interaction of Kelvin waves and non-locality of the energy transfer in superfluids. *Phys. Rev. B* **81**, 104526. (doi:10.1103/PhysRevB.81.104526)
33. Boué L, Dasgupta R, Laurie J, L'vov V, Nazarenko S, Procaccia I. 2011 Exact solution for the energy spectrum of Kelvin-wave turbulence in superfluids. *Phys. Rev. B* **84**, 064516. (doi:10.1103/PhysRevB.84.064516)
34. Shivamoggi BK. 2013 Vortex motion in superfluid ^{4}He: effects of normal fluid flow. *Eur. Phys. J. B* **86**, 275. (doi:10.1140/epjb/e2013-40099-x)
35. Cheng DK, Cromar WM, Donnelly RJ. 1973 Influence of an axial heat current on negative-ion trapping in rotating helium II. *Phys. Rev. Lett.* **31**, 433–436 (doi:10.1103/PhysRevLett.31.433)
36. Glaberson WI, Johnson WW, Ostermeier RM. 1974 Instability of a vortex array in He II. *Phys. Rev. Lett.* **33**, 1197–1200 (doi:10.1103/PhysRevLett.33.1197)
37. Ostermeier RM, Glaberson WI. 1975 Instability of vortex lines in the presence of axial normal fluid flow. *J. Low Temp. Phys.* **21**, 191–196 (doi:10.1007/BF01141298)
38. Salman H. 2013 Breathers on quantized superfluid vortices. *Phys. Rev. Lett.* **111**, 165301. (doi:10.1103/PhysRevLett.111.165301)